Structural properties of transition-metal clusters via force-biased Monte Carlo and *ab initio* calculations: A comparative study

Dil K. Limbu,[1,*] Raymond Atta-Fynn,[2,†] David A. Drabold,[3,‡] Stephen R. Elliott,[4,§] and Parthapratim Biswas[1,‖]

[1]*Department of Physics and Astronomy, The University of Southern Mississippi, Hattiesburg, Mississippi 39406, USA*

[2]*Department of Physics, University of Texas at Arlington, Arlington, Texas 76019, USA*

[3]*Department of Physics and Astronomy, Ohio University, Athens, Ohio 45701, USA*

[4]*Department of Chemistry, University of Cambridge, Cambridge CB2 1EW, United Kingdom*

(Received 17 September 2017; published 16 November 2017)

We present a force-biased Monte Carlo (FMC) method for structural modeling of the transition-metal clusters of Fe, Ni, and Cu with sizes of 13, 30, and 55 atoms. By employing the Finnis-Sinclair potential for Fe and the Sutton-Chen potential for Ni and Cu, the total energy of the clusters is minimized using the local gradient of the potentials in Monte Carlo simulations. The structural configurations of the clusters, obtained from the biased Monte Carlo approach, are analyzed and compared with the same configurations from the Cambridge Cluster Database (CCD) upon relaxation of the clusters using the first-principles density-functional code NWCHEM. The results show that the total-energy value and the structure of the FMC clusters are essentially identical to the corresponding value and the structure of the CCD clusters. A comparison of the NWCHEM-RELAX FMC and CCD structures is presented by computing the pair-correlation function, the bond-angle distribution, the coordination number of the first-coordination shell, and the Steinhardt bond-orientational order parameter, which provide information about the two- and three-body correlation functions, the local bonding environment of the atoms, and the geometry of the clusters. An atom-by-atom comparison of the FMC and CCD clusters is also provided by superposing one set of clusters onto another, and the electronic properties of the clusters are addressed by computing the density of electronic states.

DOI: 10.1103/PhysRevB.96.174208

I. INTRODUCTION

In recent years, there has been rapid progress in the development of global optimization techniques, which encompass techniques from state-of-the-art evolutionary computing [1] to the population-based swarm intelligence and differential-evolution approaches [2,3]. Despite this development, Monte Carlo (MC) methods, based on simple Metropolis and related algorithms, continue to play a major role in addressing optimization problems in science and technology. In the context of structural modeling of amorphous solids [4–6] on the atomistic length scale, the Monte Carlo procedure is particularly useful for optimization of a total-energy functional without any knowledge of atomic forces or local gradients of the energy functional. Since calculations of local gradients are computationally more complex than the evaluation of the total energy of a system, MC methods are often preferred in many optimization problems where local gradients are either not available (e.g., for a discrete or nonsmooth optimization problem) or computationally too prohibitive to compute. However, the computational advantage of the MC methods is often offset by their slow convergence behavior, which requires a longer simulation time to produce results with the desired accuracy when compared to the Newton-like and conjugate-direction methods. Recent works on structural modeling of amorphous materials using reverse Monte Carlo (RMC) simulations have indicated that atomic forces can be profitably used in RMC simulations to improve the structural quality of amorphous configurations and the efficiency of the resultant methods [7–9]. Toward that end, the main purpose of this paper is to explore the usefulness of employing local gradients (of a potential) or atomic forces in Monte Carlo simulations and to apply the method in determining the most stable structure of transition-metal (TM) clusters containing several tens of atoms. In this paper, we present a modified version of the gradient-based Monte Carlo method, originally introduced by Rossky *et al.* [10,11], to optimize transition-metal clusters and compare the results with the putative global minima of the clusters reported in the recent literature [13,14]. In particular, we compare the total energy and structures of the transition-metal clusters of Fe, Ni, and Cu from a force-biased Monte Carlo (FMC) method with those from the Cambridge Cluster Database (CCD). The latter provides the structures of the putative global minima of a number of transition-metal clusters obtained by Doye and Wales [14,15]. These authors employed an improved version of the basin-hopping algorithm of Li and Scheraga [16] to obtain the global minima of a number of transition-metal clusters using Monte Carlo simulations, coupled with conjugate-gradient optimizations. In the following, we refer to these clusters as CCD clusters and use them as a benchmark for a comparison of the total energy and structures of Fe, Ni, and Cu clusters obtained from the FMC simulations presented here. We also examine the stability of the classical FMC structures by perturbing and relaxing the clusters using a first-principles total-energy functional within the framework of the density-functional theory (DFT).

The plan of this paper is as follows. In Sec. II, we briefly review the results on the structure of the transition-metal

*dil.limbu@usm.edu
†attafynn@uta.edu
‡drabold@ohio.edu
§sre1@cam.ac.uk
‖Corresponding author: partha.biswas@usm.edu

clusters of Fe, Ni, and Cu from classical, semiclassical, and *ab initio* density-functional calculations. Section III presents the computational method associated with the implementation of atomic forces in Monte Carlo simulations used in this work. The first-principles total-energy relaxation of the structures, using the density-functional code NWCHEM [17], is also described in this section. In Sec. IV, we discuss the results from the classical FMC and *ab initio* simulations with particular emphasis on the total energy, the two- and three-body correlation functions, the atomic-coordination numbers, the bond-orientational order parameter, and the three-dimensional distribution of the atoms in the FMC and CCD clusters. This discussion is followed by the conclusion of the work in Sec. V.

II. STRUCTURE OF TRANSITION-METAL CLUSTERS: AN OVERVIEW

Transition-metal clusters have been studied extensively from computational [13–16,18–37] and experimental [38–43] points of view. They have potential applications in catalysis [44–46], magnetic-recording materials [47], carbon nanotubes [12,48], and biological applications involving genetic sequencing [49,50]. Theoretical efforts to study transition-metal clusters range from genetic algorithms [51–55] and Monte Carlo and molecular-dynamics simulations, using classical [56–61] and semiclassical [18,62–64] potentials, to *ab initio* density-functional calculations [23–35,37]. Of particular interest are the structure of Fe clusters obtained from the Finnis-Sinclair (FS) potential [65,66] and that of Ni and Cu clusters bound by the Sutton-Chen (SC) potential [67]. Similarly, the Gupta potential [22] has been extensively used to study the stable isomers and the corresponding geometry of a number of transition-metal clusters in several studies [57,61,68,69]. The putative global minima of Ni and Cu clusters have been studied extensively by Doye and Wales [14] using the Sutton-Chen potential. Likewise, Elliott *et al.* [13] have addressed the computation of the global minima of Fe clusters using the Finnis-Sinclair potential. Transition-metal clusters have also been studied using tight-binding molecular-dynamics (TBMD) simulations [18,62–64]. Lathiotakis *et al.* [18] studied Ni_n clusters ($n = 11$–55) using TBMD simulations to study the relative stability of the icosahedral and fcc structures and found that the relaxed icosahedral structure was more stable than the cuboctahedral structure for 13-atom and 55-atom clusters. This observation is consistent with the tight-binding studies of Ni and Cu clusters by other researchers [63,64], where the most stable structure of M_{13} (M = Ni, Cu) was found to be an icosahedron. An extensive analysis of the results from numerous classical and semiclassical studies appears to indicate a general trend that, at small sizes, the icosahedral motif is the preferred ground-state structure, whereas large clusters tend to adopt the structure of a truncated octahedron and a truncated decahedral structure follows in the intermediate range [38]. This observed trend has been found to be consistent with the thermodynamics of small systems and the shell structure of atoms in clusters, which take into account the internal strain, symmetries or the lack thereof, and the volume and surface dependence of the binding energy of clusters in the formation of stable structures [38].

While classical and semiclassical approaches can approximately address the evolution of the most stable structure with varying cluster sizes, any electronic effects that arise from the outer shell (valence) electrons of the atoms cannot be treated within these approaches. This is particularly relevant for the transition-metal clusters, where the presence of localized d orbitals can add further complication. For example, recent *ab initio* studies on small Au clusters have shown that the hybridization between $6s$ and $5d$ orbitals, due to strong relativistic effects, can play a significant role in determining the degree of planarity (of a structure), stability, and energetics of Au nanocluster formation [70,71].

Ab initio density-functional methods have been used extensively to study transition-metal clusters, especially 13-atom clusters of $3d/4d$ series, in the last two decades [23–37]. However, the DFT results vary considerably among research groups depending upon the type of the basis functions and the nature of the exchange-correlation (XC) functional employed in the calculations and the method used to sample candidate structures from the potential-energy surface (PES) during simulations. While a number of low-energy structures have been proposed as possible ground-state structures for 13-atom TM clusters, there is still no consensus among the researchers in the community. Using density-functional calculations, Oviedo and Palmer [25] reported the presence of a number of "amorphous" low-energy isomers of M_{13} (M = Cu, Ag, and Au) with a total energy difference of 0–1 eV from each other. The authors noted that the cuboctahedral structure was more stable than the icosahedral structure for the ground-state structure of Ag_{13}, an observation which is at variance with the results from recent *ab initio* studies [30–32,35]. Chang and Chou [26] studied 13-atom clusters of early and late transition-metal series using the plane-wave density-functional code VASP [72]. The results suggest that a buckled biplanar (BBP) [73] structure is more stable than the icosahedral structure when the d shell is more than half filled. The BBP structure was found to be the most stable structure for 13-atom Ag and Cu clusters in their study, which were 0.84 and 0.53 eV lower than the corresponding icosahedral structure, respectively. While this observation is supported by the DFT studies of Longo and Gallego [28] and Wang and Johnson [30], a number of Gaussian-orbital- and plane-wave-based DFT studies [31,32,35] reported different structures for Ag_{13} and Cu_{13} clusters. A similar observation applies to the Ni_{13} structure. Pseudoatomic-orbital-based DFT studies [28,33] suggest that the icosahedral structure is the most stable for Ni_{13}, but a number of researchers dispute this observation by proposing new structures based on plane-wave-based DFT calculations [31,35–37].

In summary, while empirical and semiempirical studies can predict some trends in cluster morphology with increasing cluster sizes, it is difficult to predict accurately the ground-state structure of many transition-metal clusters without explicitly taking into account quantum-mechanical effects in the calculations. On the other hand, the density-functional approach can address the problem fairly accurately, but a few theoretical issues concerning the use of an appropriate XC functional and the need for the inclusion of the semicore states in the pseudopotential for specific systems (e.g., V and Cr) continue to exist (see, for example, Refs. [34,74]).

TABLE I. Parameters for the Finnis-Sinclair [65,66] (for Fe) and Sutton-Chen [67] potentials.

	n	m	a (Å)	ϵ (eV)	γ	c (Å)	c_o	c_1	c_2
Fe			3.569745	1.828905	1.8	3.40	1.2371147	−0.3592185	−0.0385607
Ni	9	6	3.52	0.015707			39.432		
Cu	9	6	3.61	0.012382			39.432		

III. COMPUTATIONAL METHOD

The starting point of our method is to generate a random configuration such that no two atoms are at a distance closer than twice the diameter of the constituent atoms. The total energy of an atomic configuration can be calculated by using an appropriate classical potential. In particular, we employ the FS potential [65,66] for Fe clusters and the SC potential [67] for Ni and Cu clusters. The corresponding potential parameters are listed in Table I. The Finnis-Sinclair potential, for a system consisting of N atoms, is written as

$$E = \frac{1}{2}\sum_{i}^{N}\sum_{j\neq i}^{N} V(r_{ij}) - \epsilon\sum_{i}^{N}\sqrt{\rho_i}. \tag{1}$$

The repulsive two-body interaction $V(r_{ij})$ and the attractive on-site energy ρ_i are given by

$$V(r_{ij}) = \begin{cases} (r_{ij}-c)^2\left(c_o + c_1 r_{ij} + c_2 r_{ij}^2\right) & \text{for } r_{ij} \leqslant c, \\ 0 & \text{for } r_{ij} > c, \end{cases} \tag{2}$$

and

$$\rho_i = \sum_{j\neq i}^{N} \phi(r_{ij}), \tag{3}$$

respectively, where

$$\phi(r_{ij}) = \begin{cases} (r_{ij}-a)^2 + \gamma\frac{(r_{ij}-a)^3}{a} & \text{for } r_{ij} \leqslant a, \\ 0 & \text{for } r_{ij} > a. \end{cases} \tag{4}$$

The Sutton-Chen potential is given by

$$E = \epsilon\sum_{i}^{N}\left[\frac{1}{2}\sum_{j\neq i}^{N}\left(\frac{a}{r_{ij}}\right)^n - c_o\sqrt{\rho_i}\right], \tag{5}$$

where

$$\rho_i = \sum_{j\neq i}^{N}\left(\frac{a}{r_{ij}}\right)^m. \tag{6}$$

In our approach, the initial random configuration was equilibrated at a temperature $T = 3000$ K for 10^5 Monte Carlo steps (MCS). Subsequently, the temperature of the system was decreased sequentially by a factor of 0.99, and at each temperature, the system was equilibrated for 10^5 MCS until the final temperature of the system was reduced to 1 K. The total-energy relaxation was achieved in two steps: (a) computing the total force on each atom $\mathbf{f_i^n}$ in the initial state $\mathbf{n}$ and (b) displacing a randomly selected atom at site i from an initial state $\mathbf{n}$ to a proposed state $\mathbf{m}$ by [10,75]

$$\Delta\mathbf{r_i^{mn}} = \alpha\,\delta\mathbf{r_i^{mn}} + \beta\,A\,\mathbf{f_i^n}. \tag{7}$$

The parameters α and A in Eq. (7) determine the length of a random displacement $\alpha\,\delta\mathbf{r_i^{mn}}$ and the contribution from the potential gradient $-\mathbf{f_i^n}$ in generating a proposed configuration $\mathbf{m}$, respectively. One may treat β as an optimization parameter without any reference to temperature, or β can be simply set to $\frac{1}{k_B T}$, where k_B is the Boltzmann constant. The displacement $\delta\mathbf{r_i^{mn}}$ is generally, but not necessarily, drawn from a Gaussian distribution with a zero mean and a variance $2A$. It can be shown that the prescription stated in Eq. (7) is related to Brownian-dynamics simulations in the presence of an external force for an appropriate choice of $\alpha\,\delta\mathbf{r_i^{mn}}$ and A, where the motion of a particle is governed by the sum of the external force(s) and a random force reflecting the complex interaction between the particle and a noisy environment. Following Rossky *et al.* [10] and Allen and Tildesley [11], one can show that a proposed MC move in Eq. (7) is accepted with the probability $P_{mn} = \min[1, \exp(-\beta\,\Delta E_i^{mn})]$, where

$$\Delta E_i^{mn} = \delta E^{mn} + \left[\frac{1}{2}\left(\mathbf{f_i^n} + \mathbf{f_i^m}\right)\cdot\Delta\mathbf{r_i^{mn}} + \frac{\beta A}{4}\left\{\left(\delta\mathbf{f_i^{mn}}\right)^2 + 2\mathbf{f_i^n}\cdot\delta\mathbf{f_i^{mn}}\right\}\right] \tag{8}$$

and

$$\delta E^{mn} = E^m - E^n, \quad \delta\mathbf{f_i^{mn}} = \mathbf{f_i^m} - \mathbf{f_i^n}.$$

In Eq. (8), E^n and E^m are the total energy of the system in the initial state and that in the proposed state, respectively. Likewise, $\mathbf{f_i^n}$ and $\mathbf{f_i^m}$ are the total force on an atom at site i before and after the displacement, respectively. An MC move is accepted or rejected using the conventional Metropolis algorithm. In this work, we chose to move one atom at a time, but it is possible to move a group of atoms simultaneously by ensuring that the change in total energy ΔE^{mn}, associated with multiatom moves, is properly evaluated. To improve the acceptance rate, we adjusted the step length by assuming a linear temperature dependence of α with a lower cutoff value of 0.001 Å at 1 K and an upper cutoff value of 0.05 Å at 3000 K. The value of A was chosen in such a way that βA was approximately $4\text{–}5 \times 10^{-3}$ and $\delta\mathbf{r_i^{mn}}$ was a random number (between -1 and $+1$) taken from a uniform distribution [76]. In this preliminary study, we made no attempts to optimize the values of α and A apart from what we have stated above. These parameters can be further adjusted during simulations to improve the efficiency of the method.

To examine the stability of the structure at the putative global minimum of a classical potential, namely, the Finnis-Sinclair or the Sutton-Chen potential in the present study, we have carried out *ab initio* total-energy optimizations of the CCD clusters and those obtained from our FMC simulations.

TABLE II. Total energy of Cu, Ni, and Fe clusters from the classical FMC simulation along with the corresponding value of the CCD clusters.

System	FMC (eV)	CCD (eV)	$E_{fmc}-E_{ccd}$ (meV)
Fe_{13}	− 40.2983	− 40.2985	0.2
Fe_{30}	− 101.4469	− 101.4513	4.4
Fe_{55}	− 194.6847	− 194.6868	2.1
Ni_{13}	− 44.1142	− 44.1143	0.1
Ni_{30}	− 108.4284	− 108.4296	1.2
Ni_{55}	− 207.6107	− 207.6135	2.8
Cu_{13}	− 34.7757	− 34.7758	0.1
Cu_{30}	− 85.4753	− 85.4762	0.9
Cu_{55}	− 163.6617	− 163.6640	2.3

Ab initio calculations proceed within the framework of density-functional theory [77] using a plane-wave basis, as implemented in the DFT code NWCHEM [17]. For this purpose, a cluster was placed in a large cubic supercell such that the neighboring images of the cluster do not interact with each other in order to prevent the system from being treated as a bulk solid during *ab initio* relaxations. A cubic supercell with a length of 20 Å was found to be sufficient for the present calculations. The exchange-correlation energy was treated using the generalized gradient approximation (GGA) in the Perdew-Burke-Ernzerhof (PBE) formulation [78], and the norm-conserving pseudopotentials, modified into a separable form due to Kleinman and Bylander [79], were employed in this work. The Kohn-Sham eigenstates were expanded in a plane-wave basis with a kinetic-energy cutoff of 37 hartrees (1006.8 eV). To verify the sufficiency of the energy cutoff, a few clusters were tested using a high-energy cutoff of 45 hartrees (1224.5 eV), which yielded no significant changes in the geometry and the total-energy values of the clusters in comparison to the results obtained by using a cutoff value of 37 hartrees. Throughout this work, the total-energy optimization of the clusters was carried out using the spin-polarized PBE-GGA functional until the total force on each atom of the clusters was found to be less than 0.01 eV/Å. In addition, Car-Parrinello molecular-dynamics (CPMD) [80] simulations and subsequent geometry relaxations were used to check the thermal stability of the 13-atom Cu/Ni/Fe clusters.

IV. RESULTS AND DISCUSSION

A. Global minima from the classical FMC simulations

We begin by addressing the total energy of the putative global minima of the clusters from the classical FMC simulations and then proceed to compare the results with the corresponding data from the CCD [81]. In Table II, we list the total energy of 13-, 30-, and 55-atom clusters of Fe, Ni, and Cu from the classical FMC simulations along with the corresponding CCD values. A direct comparison of the total-energy values, from the second and third columns in Table II suggests that the FMC values practically coincide with the CCD values except for Fe_{30}, where a deviation as small as 4.4 meV has been observed. This deviation is significantly smaller than the energy associated with the thermal fluctuations at 300 K. Notwithstanding the observation that the CCD energy values are consistently lower than the corresponding FMC values by about 0–5 meV, the FMC results are quite impressive considering the fact that no gradient optimization has been performed on the FMC structures. This reflects the simplicity and efficiency of the FMC method. The latter is apparent from Figs. 1(a) and 1(b), where the evolution of the total energy with the CPU time and the number of the MC steps are plotted, respectively. It is apparent from Fig. 1(a) that the total-energy decay in the FMC simulation is sufficiently faster than its MC counterpart despite the fact that computationally expensive local gradients or atomic forces have been evaluated during the FMC simulation. A similar observation follows from the evolution of the total energy with the MC steps in Fig. 1(b).

To examine the stability of the clusters at the putative global minimum of the FS and SC potentials, we list in Table III the total-energy values obtained from the first-principles relaxations of the classical FMC and CCD configurations using the density-functional code NWCHEM by perturbing the atomic positions by up to 15% of the average nearest-neighbor distance between the atoms. Table III suggests that the total-energy differences are quite small, with a deviation less than one tenth of an electron volt, except for 55-atom clusters. A deviation of 0.1–0.16 eV has been observed for 55-atom clusters, which is due partly to the difficulty in optimizing large clusters using the computationally expensive CPMD method and in part to the spin-polarized nature of the calculations. It may be noted that the total-energy values of the 30-atom NWCHEM-RELAX FMC clusters for all but Cu_{30} are consistently lower than the corresponding CCD values and vice versa for

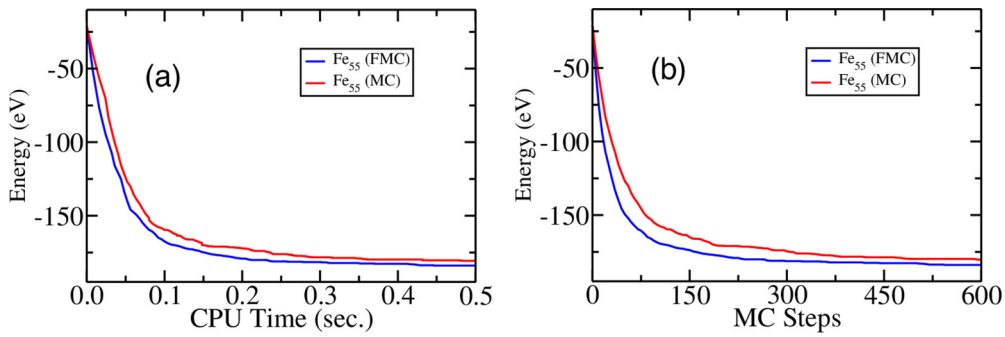

FIG. 1. The evolution of the total energy of an Fe_{55} cluster in the classical FMC and MC simulations. (a) Total energy versus CPU time. (b) Total energy versus MCS.

TABLE III. Total energy of Fe, Ni, and Cu clusters from *ab initio* relaxation of the FMC and CCD structures.

System	FMC[a] (hartrees)	CCD[a] (hartrees)	$E_{fmc}-E_{ccd}$ (eV)
Fe_{13}	− 1575.6009	− 1575.6018	0.0245
Fe_{30}	− 3636.0472	− 3636.0366	− 0.288
Fe_{55}	− 6666.4826	− 6666.4886	0.163
Ni_{13}	− 556.1933	− 556.1940	0.019
Ni_{30}	− 1283.9900	− 1283.9883	− 0.0463
Ni_{55}	− 2354.5115	− 2354.5154	0.106
Cu_{13}	− 707.5190	− 707.5205	0.041
Cu_{30}	− 1633.1592	− 1633.1603	0.032
Cu_{55}	− 2994.5459	− 2994.5497	0.103

[a]One hartree = 27.211 eV.

the clusters with 55 atoms. In view of this observed energy difference, it would be instructive to examine to what extent this small energy variation can affect the three-dimensional structure of the clusters. We address this question in Secs. IV C and IV D with an emphasis on the two-, three-, and higher-order correlation functions and compare the real-space distribution of the atoms obtained from the NWCHEM-RELAX FMC and CCD clusters.

B. Structure of 13-atom Cu/Ni/Fe clusters from *ab initio* studies

Our discussion in Sec. II suggests that the electronic effects arising from the *d* electrons can play a significant role in the determination of the ground-state structure of a number of 13-atom TM clusters, such as Cu and Fe. The great majority of the simulation studies on TM clusters using classical potentials suggest that the icosahedral structure is the preferred minimum for the 13-atom clusters of Cu and Fe, but quite a few *ab initio* studies indicate that these systems adopt a biplanar or platelet-like form, instead of a more symmetrical icosahedral structure. Even within the density-functional framework, the results vary considerably from one study to another. For example, the plane-wave-based DFT calculations, using VASP, by Chang and Chou [26] suggest that a BBP structure of Ag_{13} and Cu_{13} is more stable than the corresponding icosahedral structure. However, the results from the Gaussian-orbital-based DFT calculations by Pereiro *et al.* [31] indicate that the icosahedral structure is the most stable structure of Ag_{13}. The results above

TABLE IV. *Ab initio* total-energy values of 13-atom transition-metal clusters from a joint FMC-NWCHEM simulation. For Cu_{13}, the energy difference $\Delta E = E - E_{\min}$ is expressed with respect to the lowest-energy configuration. ICO = icosahedral.

Cluster	Initial symmetry	Final symmetry	E (hartrees)	ΔE (eV)
Ni	ICO	ICO	−556.1921	
Fe	ICO	ICO	−1575.6020	
Cu	BBP	bilayer 1	−707.5611	0.31
	ICO	bilayer 2	−707.5723	0.0
	HBL	bilayer 3	−707.5653	0.19

contrast with those based on the plane-wave DFT studies, using VASP, by Hue *et al.* [32] and Piotrowski *et al.* [35], which reported new ground-state structures of Ag_{13}. Furthermore, recent *ab initio* studies on TM clusters by Jena *et al.* [82,83], using VASP [72] and GAUSSIAN [84], have indicated that the ground-state energy of 13-atom Cu/Ni/Fe clusters correspond to well-defined spin multiplicities, which need to be taken into account for accurate total-energy calculations of 13-atom Cu/Ni/Fe clusters. Thus, the structures of some of the 13-atom TM clusters are still very controversial, and there is a need for accurate *ab initio* calculations for structural determination of small TM clusters. Since an in-depth study of 13-atom TM clusters is outside the scope of the present work, we specifically address here the credibility of the structures of a few 13-atom TM clusters, which are obtained from the classical FMC simulations followed by CPMD [80] and first-principles total-energy relaxation using the density-functional code NWCHEM. Here, we have used the values of spin multiplicities reported in Ref. [82].

In Table IV, we list the total-energy values of 13-atom Cu, Ni, and Fe clusters obtained from the joint FMC-NWCHEM simulations. Starting with the 13-atom icosahedral structure obtained from the classical FMC simulations, the total energy of each cluster was minimized using the density-functional code NWCHEM. Thereafter, finite-temperature CPMD simulations were carried out at $T = 300$ K for 6–10 ps, with a time step of 0.12 fs, to explore the neighboring regions of the potential-energy surface, followed by total-energy relaxation to determine the equilibrium structure of the clusters. An examination of the final structures reveals that Ni_{13} and Fe_{13} continue to remain in the icosahedral structure, whereas Cu_{13} transforms

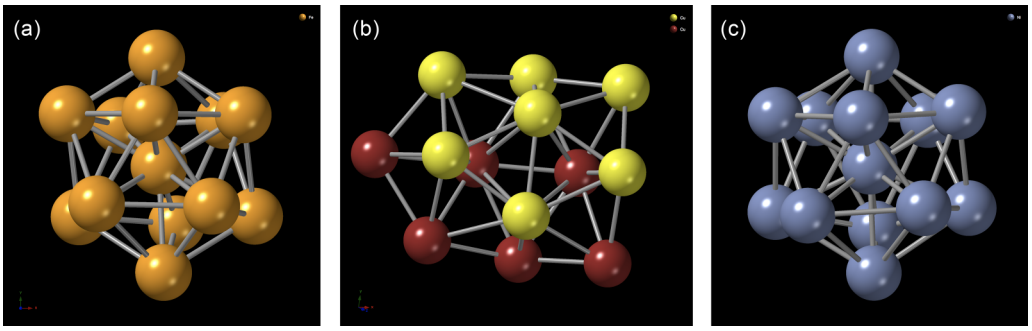

FIG. 2. The putative ground-state structures of 13-atom transition-metal clusters from a joint FMC-NWCHEM simulation: (a) Fe_{13} (icosahedron), (b) Cu_{13} (bilayer 2) with a buckled hexagonal layer (yellow), and (c) Ni_{13} (icosahedron). See Table IV for the ground-state energy of the structures and the possible low-energy isomers of Cu_{13}.

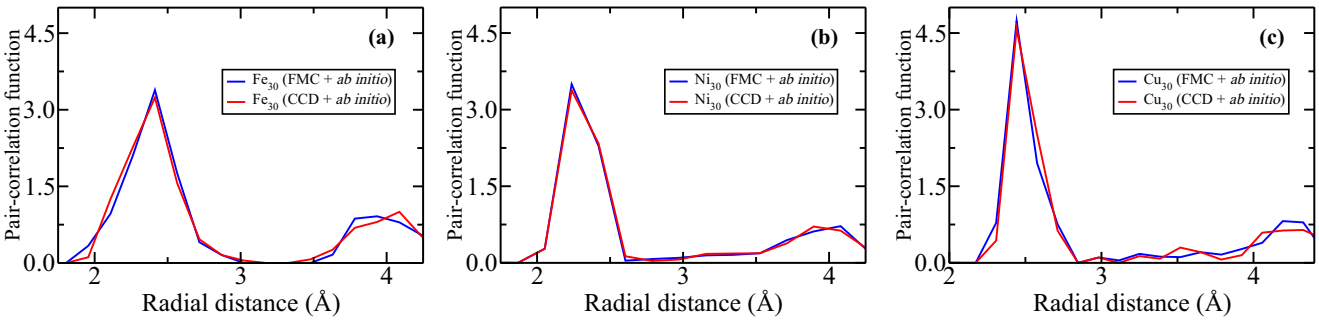

FIG. 3. The pair-correlation functions of (a) Fe_{30}, (b) Ni_{30}, and (c) Cu_{30} clusters obtained from *ab initio* relaxations of FMC (blue) and CCD (red) structures using the density-functional code NWCHEM.

from the icosahedral structure to a BBP structure during 10 ps of thermalization (at 300 K) and eventually adopts a low-energy bilayer structure upon post-CPMD total-energy relaxation. To further examine the stability of the bilayer structure of Cu_{13}, additional CPMD runs were conducted for 10 ps starting with a BBP structure and a hexagonal bilayer (HBL) structure [73]. In both cases, the simulations produced bilayer structures which were energetically very close to each other but slightly different in structure. Table IV lists the total energy of the clusters, the initial and final symmetries, and the energy difference ΔE between the bilayer structures of Cu_{13}. Figure 2 shows the minimum-energy structures of the 13-atom Cu, Ni, and Fe clusters, obtained from the joint FMC-NWCHEM runs, of 6–10-ps duration, followed by total-energy relaxations. The presence of a buckled hexagonal layer with a central atom, shown in yellow, is clearly visible in Fig. 2(b). The remaining atoms form a highly distorted layer to produce an approximate bilayer or plateletlike structure. On the other hand, the 13-atom Ni and Fe clusters are found to be stable in the icosahedral structure, as shown in Figs. 2(a) and 2(c), respectively. The transition of the Cu_{13} cluster from a 13-atom icosahedral structure to a BBP structure and then to a bilayer structure indicates that, for an exhaustive molecular-dynamical search for new structures on the PES, one must conduct rather long simulations lasting several tens of picoseconds at different temperatures.

C. Local atomic structure and bonding environment

Since the ground-state configuration of a cluster must be independent of the optimization method for a given potential, it is appropriate to examine whether a small difference in the total energy between a pair of clusters, mentioned in Sec. IV A, can have nontrivial effects on the three-dimensional distribution of the atoms. This is particularly relevant for large clusters due to the presence of a multitude of low-lying minima on the potential-energy surface. For large clusters, it is possible for the system to adopt a number of different structural configurations, which are either energetically degenerate or very close to each other (also known as an isomer). Thus, it is necessary to examine the structural similarities and differences between the NWCHEM-RELAX FMC and CCD clusters by systematically addressing the atomic-correlation functions of increasing order. Since the number density of a cluster can vary with its size, we have assumed a suitable bounding box for the computation of the pair-correlation function of a cluster of given size [85]. Figure 3 presents the pair-correlation functions (PCFs) for a 30-atom cluster of Fe, Ni, and Cu, obtained from the NWCHEM-RELAX FMC and CCD configurations. It is apparent from Fig. 3 that, apart from a minute difference in the vicinity of 4 Å for Fe and Cu clusters, the PCFs of the FMC and CCD clusters effectively coincide with each other, reflecting the structural similarities as far as the radial correlation of the atoms is concerned. Similar conclusions can be reached from Fig. 4, where the distribution of the bond angles between the nearest-neighbor atoms is presented.

Further characterization of the clusters is possible by analyzing the distribution of the first-shell coordination numbers of the atoms. To this end, we define the nearest-neighbor distance between the atoms from the first minimum of the pair-correlation functions, as shown in Fig. 3. For Fe_{30}, Ni_{30}, and Cu_{30} clusters, these values correspond to 3.2, 2.65, and 2.9 Å, respectively. The values are consistent with

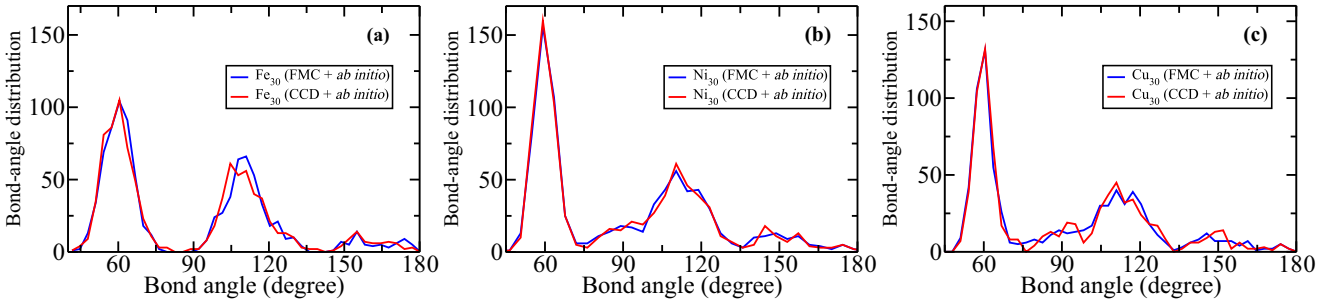

FIG. 4. The distribution of the nearest-neighbor bond angles for (a) Fe_{30}, (b) Ni_{30}, and (c) Cu_{30} clusters. The results for the FMC and CCD structures, after relaxation using NWCHEM, are shown in blue and red, respectively.

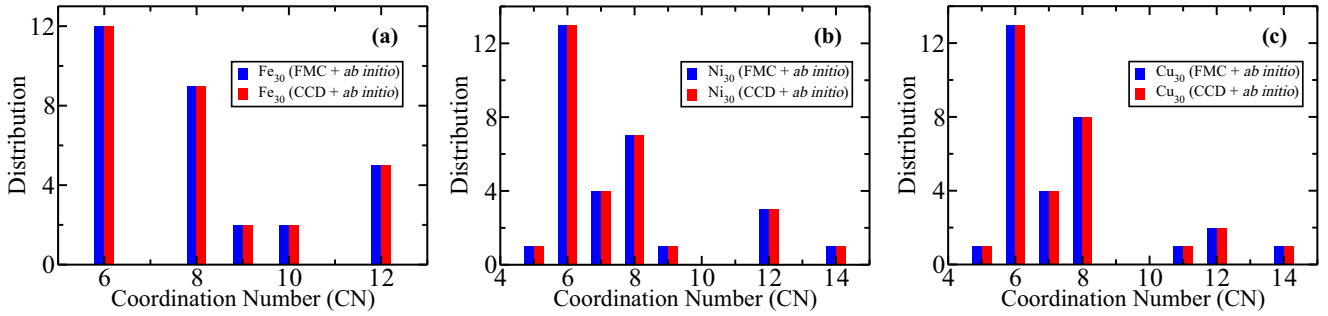

FIG. 5. Histograms showing the coordination numbers of the first-shell atoms in (a) Fe_{30}, (b) Ni_{30}, and (c) Cu_{30} clusters. The FMC-NWCHEM and CCD-NWCHEM configurations are indicated in the plots.

the sum of the atomic radius of the constituent atoms in the clusters. Figure 5 shows the histograms of the first-shell atomic-coordination numbers of Fe_{30}, Ni_{30}, and Cu_{30} clusters, obtained from the NWCHEM-RELAX FMC and CCD configurations.

D. Bond-orientational order parameter

In the preceding section, we showed that the radial and bond-angle distributions, as well as the atomic-coordination numbers, of the NWCHEM-RELAX FMC and CCD clusters closely match each other. However, this does not necessarily establish that the FMC and CCD clusters are identical to each other as far as the three-dimensional distribution of the atoms is concerned. For example, for a given set of atoms, it is possible to construct different local-bonding environments that can have identical radial, bond-angle, and atomic-coordination number distributions. Thus, to obtain information on the orientation of a set of bonds (with respect to a fixed coordinate system in space) formed by a group of atoms, an appropriate bond-orientational order parameter (BOP) needs to be defined. To this end, we compute the BOP, introduced by Steinhardt *et al.* [86], in an effort to further establish that the FMC and CCD clusters are nearly identical to each other. Since the BOP depends on the number of nearest neighbors and the relative orientations of the neighbors with respect to the central atom, it incorporates some aspects of structural information from higher-order correlation functions of the clusters. The Steinhardt BOP often provides a simple and effective measure for determining the presence of micro- or paracrystalline structural units in solids. The local BOP Q_l^i reflects the bonding environment of an atom at site i, which is associated with the orientation of a set of bonds that originate from site i and terminate at its nearest neighbors. While Q_l^i is independent of the bond lengths, it depends on the number of nearest neighbors of site i and their orientations with respect to a three-dimensional coordinate system with site i at its origin. In a spherical polar coordinate system, the local BOP Q_l^i is given by

$$Q_l^i = \sqrt{\frac{4\pi}{2l+1}\sum_{m=-l}^{l}\left|\frac{1}{n_i}\sum_{j\in[n_i]}Y_l^m(\theta(\mathbf{r_{ij}}),\phi(\mathbf{r_{ij}}))\right|^2},$$

and the global BOP Q_l follows from the sum of the individual values of Q_l^i at site i. Here, n_i is the number of the nearest neighbors of atom i, N is the total number of atoms in the system, and θ and ϕ are the polar and azimuthal angles of the bond $\mathbf{r}_{ij}$, respectively. The symbol $[n_i]$ indicates the atomic indices of n_i nearest neighbors of atom i, and Q_l is the site-average value of Q_l^i over all atomic sites. Different values of l generally correspond to different crystalline structures; for example, Q_4 and Q_6 are often used in the literature to distinguish a cubic structure from a hexagonal one. Figure 6 shows the bond-orientational order parameter for two sets of Fe_{30}, Ni_{30}, and Cu_{30} clusters, obtained from *ab initio* relaxations of the FMC and CCD structures using NWCHEM. The results for each set of the FMC and CCD clusters are essentially identical except for a minor deviation for Fe_{30} owing to subtle differences in the bond-angle distribution of the FMC and CCD clusters near 110°, as observed in Fig. 4(a).

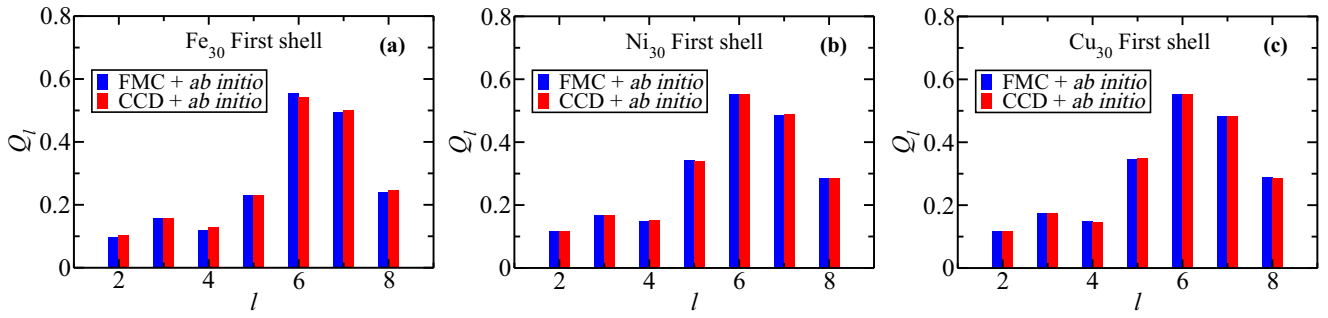

FIG. 6. Bond-orientational order parameters Q_l for (a) Fe_{30}, (b) Ni_{30}, and (c) Cu_{30} clusters for several values of l. The results for the FMC-NWCHEM and CCD-NWCHEM structures are shown in blue and red, respectively.

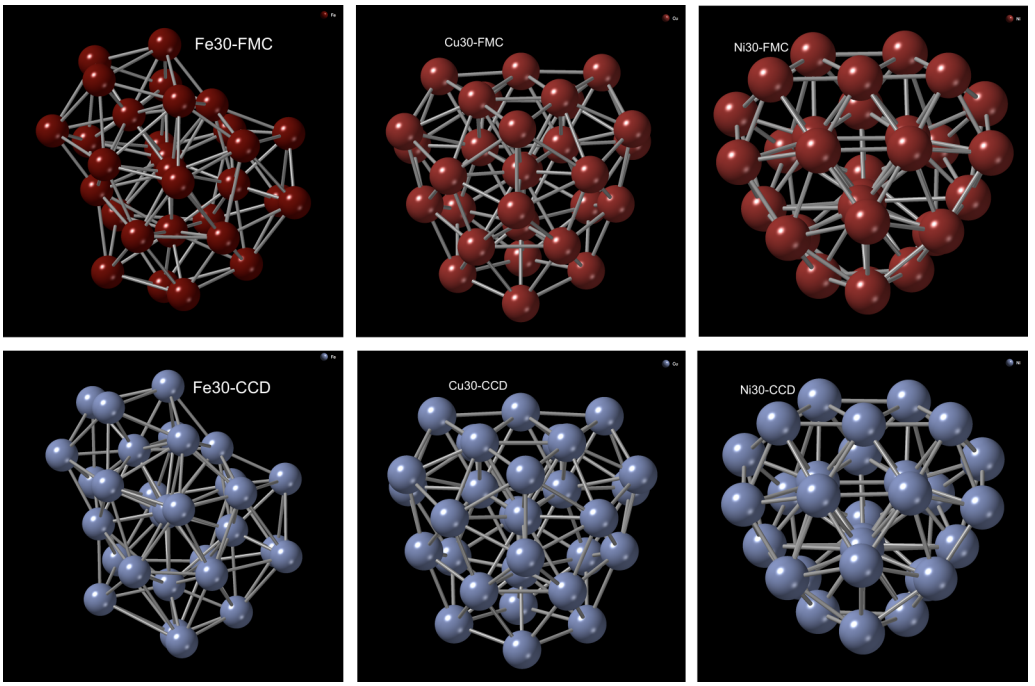

FIG. 7. Geometry of Fe_{30}, Ni_{30}, and Cu_{30} clusters obtained from *ab initio* NWCHEM relaxations of the FMC (top panel) and CCD (bottom panel) clusters. For comparison, each configuration was subjected to a translation and appropriate rotations, as described in the text.

E. Geometry of transition-metal clusters

Having established that the two- and three-body correlation functions, as well as the local structure and the bonding environment of the atoms, of the FMC and CCD clusters practically match each other, it seems intuitively valid to state that the clusters are essentially identical. However, a rigorous justification of this statement, based on the results discussed so far, turns out to be particularly delicate owing to the hierarchy of the high-order correlation functions, and a more direct approach is needed to establish the identical nature of the FMC and CCD clusters. In an effort to achieve this, we therefore

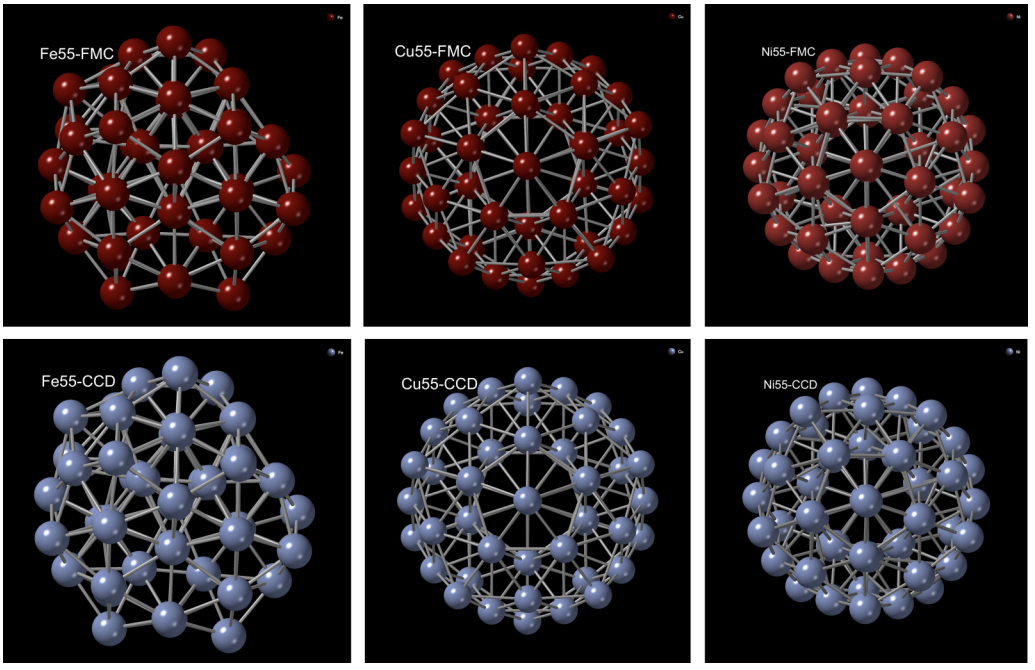

FIG. 8. The structure of 55-atom Fe, Ni, and Cu clusters obtained from the *ab initio* NWCHEM relaxation starting from the FMC and CCD configurations. The FMC (top panel) and CCD (bottom panel) clusters are shown in dark red and light blue, respectively. Each configuration was subjected to a translation and rotations for comparison.

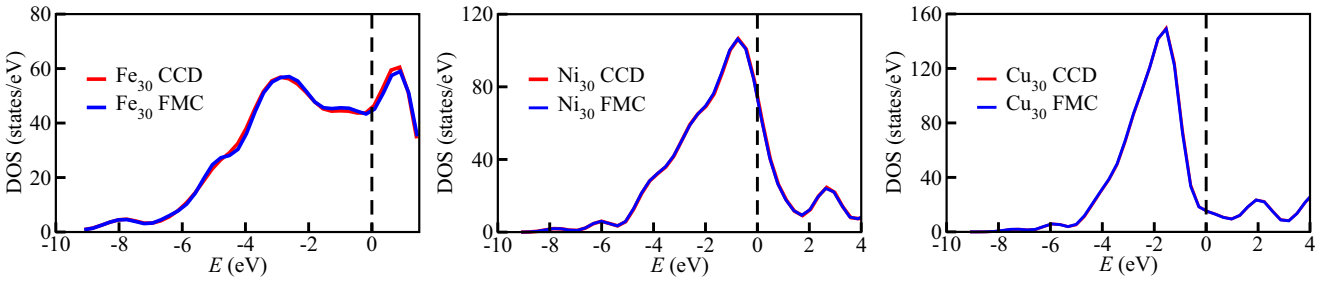

FIG. 9. Electronic densities of states of 30-atom Fe, Ni, and Cu clusters. The results for the FMC and CCD clusters are shown in blue and red, respectively. The highest-occupied energy level is shown as a dashed vertical line (black) at 0 eV. For the purpose of comparison, we have broadened the eigenvalue distributions using a Gaussian function with a broadening parameter of 0.3 eV.

proceed to compare the structures atom by atom in this section. Toward that end, our approach is based on the following assertion: given two (nearly) identical configurations, it is possible to construct a series of transformations involving translations and rotations in three dimensions such that one configuration can be (approximately) mapped onto the other. We implement this ansatz by (a) translating the center of mass (c.m.) of each configuration to (0, 0, 0), (b) subsequently finding a unique direction vector for each configuration (e.g., the direction vector from the c.m. to the nearest atom), and (c) aligning these direction vectors with the z axis (0, 0, 1) using the axis-angle representation of vector rotation in three-dimensional space [87]. We emphasize that, in order for this ansatz to work satisfactorily, the configurations must be nearly identical to each other. Since the results in the preceding sections demonstrate unambiguously that this condition is amply satisfied by the FMC and CCD clusters, we may expect that an appropriate transformation exists and that it can be employed for the purpose of superposition. Figures 7 and 8 show the geometry of 30-atom and 55-atom clusters, respectively, obtained from the joint FMC-NWCHEM relaxation. For the purpose of direct comparison with the CCD clusters, each of the FMC clusters was subjected to a translation and appropriate rotations. The resulting structures in Figs. 7 and 8 conclusively demonstrate that the FMC clusters are identical to their CCD counterparts. Finally, the electronic density of states of Fe_{30}, Ni_{30}, and Cu_{30} clusters from NWCHEM is plotted in Fig. 9. It is evident from the plots that the FMC and CCD configurations produce almost identical electronic densities of states throughout the energy spectrum. Thus, the electronic density of states of the clusters provides additional and independent corroboration that the clusters are (nearly) identical in nature.

V. CONCLUSIONS

In this paper, we have studied the most stable structures of the transition-metal clusters of Fe, Ni, and Cu using classical simulations followed by quantum-mechanical total-energy relaxations using density-functional theory. Starting from a random structural configuration, the total energy of a cluster is computed using a force-biased Monte Carlo approach, which efficiently explores the potential-energy landscape to determine the most likely configuration of the cluster at the putative global minimum and the low-energy isomers without employing any gradient-optimization techniques. Our method is illustrated using the Finnis-Sinclair potential for Fe clusters and the Sutton-Chen potential for Ni and Cu clusters, with sizes of up to 55 atoms, for which the putative global minima and the corresponding geometry of the clusters are available in the literature from a number of sophisticated gradient-based optimization methods. In particular, we have compared our results from the classical FMC simulations with the corresponding structural data obtained from the Cambridge Cluster Database. The results suggest that the classical FMC method can produce structural configurations that are essentially identical to those of the CCD configurations as far as the total energy, the pair-correlation function, the bond-angle distribution, the atomic-coordination numbers, and the bond-orientational order parameter are concerned. Atom-by-atom comparisons between the FMC and CCD clusters were presented by mapping the former onto the latter using a transformation involving a translation and suitable Euler rotations. The stability of the classical FMC clusters was examined by perturbing the atomic positions and relaxing the perturbed configurations using the first-principles density-functional code NWCHEM. *Ab initio* total-energy relaxations of the FMC clusters indicate, with the exception of 13-atom Cu cluster, that the resulting relaxed structures are practically identical to the starting FMC structures as far as the pair-correlation distribution, the bond-angle distribution, and the first-shell coordination number of the atoms are concerned. For Fe_{13} and Ni_{13} clusters, we find that the icosahedral structure is the most stable structure, whereas Cu_{13} is found to adopt a bilayer or plateletlike structure in our study.

We conclude this paper with the following observation. In this study, our *ab initio* search for new structures is by no means exhaustive as the primary goal of our work was to examine the effectiveness of the FMC approach in determining the ground-state structures of transition-metal clusters from classical potentials. Having achieved this goal, we have employed finite-temperature *ab initio* molecular-dynamics (AIMD) simulations to examine the credibility of the ground-state structure from classical potentials from the first-principles point of view. Since finite-temperature AIMD cannot adequately explore the potential-energy surface in a limited simulation time of a few tens of picoseconds, as observed in numerous DFT studies on 13-atom transition-metal clusters (see Sec. II), alternative approaches to sample structures from the potential-energy surface of the clusters are

necessary. In this paper, we have offered such an approach and have shown unambiguously that the classical version of the approach can effectively determine the putative ground-state structures of a number of small transition-metal clusters. It is appropriate to expect that an *ab initio* version of the FMC algorithm would be highly suitable for an extensive search for the ground-state structure of transition-metal clusters using total energies and forces. Finally, our method can be applied to model bulk amorphous solids using *ab initio* forces from density-functional simulations, where one is primarily interested in obtaining a set of stable atomic configurations that correspond to low-lying local minima on the potential-energy surface. In future, we will address these problems using an optimized version of the FMC algorithm.

ACKNOWLEDGMENTS

This work is partially supported by the US National Science Foundation under Grants No. DMR 1507166, No. DMR 1507118, and No. DMR 1506836. We acknowledge the use of computing resources at the Texas Advanced Computing Center. P.B. thanks Prof. D. J. Wales for providing the coordinates of Fe/Ni/Cu CCD clusters through the Cambridge Cluster Database.

[1] A. E. Eiben and J. E. Smith, *Introduction to Evolutionary Computing* (Springer, Berlin, 2003).
[2] A. P. Engelbrecht, *Computational Intelligence: An Introduction* (Wiley, Hoboken, NJ, 2007).
[3] K. Biswas, J. Chem. Phys. **147**, 104108 (2017).
[4] R. L. McGreevy, J. Phys. Condens. Matter **13**, R877 (2001).
[5] P. Biswas, G. T. Barkema, N. Mousseau, and W. F. van der Weg, Europhys. Lett. **56**, 427 (2001).
[6] P. Biswas, R. Atta-Fynn, and D. A. Drabold, Phys. Rev. B **69**, 195207 (2004).
[7] A. Pandey, P. Biswas, and D. A. Drabold, Phys. Rev. B **92**, 155205 (2015).
[8] A. Pandey, P. Biswas, and D. A. Drabold, Sci. Rep. **6**, 33731 (2016).
[9] A. Pandey, P. Biswas, B. Bhattarai, and D. A. Drabold, Phys. Rev. B **94**, 235208 (2016).
[10] P. J. Rossky, J. D. Doll, and H. L. Friedman, J. Chem. Phys. **69**, 4628 (1978).
[11] M. P. Allen and D. J. Tildesley, *Computer Simulation of Liquids* (Oxford University Press, Oxford, 1987).
[12] Y.-L. Li, I. A. Kinloch, and A. H. Windle, Science **304**, 276 (2004).
[13] J. A. Elliott, Y. Shibuta, and D. J. Wales, Philos. Mag. **89**, 3311 (2009).
[14] J. P. K. Doye and D. J. Wales, New J. Chem. **22**, 733 (1998).
[15] D. J. Wales and J. P. K. Doye, J. Phys. Chem. A **101**, 5111 (1997).
[16] Z. Li and H. A. Scheraga, Proc. Natl. Acad. Sci. USA **84**, 6611 (1987).
[17] M. Valiev, E. Bylaska, N. Govind, K. Kowalski, T. Straatsma, H. V. Dam, D. Wang, J. Nieplocha, E. Apra, T. Windus, and W. de Jong, Comput. Phys. Commun. **181**, 1477 (2010).
[18] N. N. Lathiotakis, A. N. Andriotis, M. Menon, and J. Connolly, Europhys. Lett. **29**, 135 (1995).
[19] V. G. Grigoryan and M. Springborg, Chem. Phys. Lett. **375**, 219 (2003).
[20] C. Luo, New J. Phys. **4**, 10 (2002).
[21] J. M. Montejano-Carrizales, M. P. Iñiguez, J. A. Alonso, and M. J. López, Phys. Rev. B **54**, 5961 (1996).
[22] R. P. Gupta, Phys. Rev. B **23**, 6265 (1981).
[23] C. Massobrio, A. Pasquarello, and R. Car, Chem. Phys. Lett. **238**, 215 (1995).
[24] P. Calaminici, A. M. Köster, N. Russo, and D. R. Salahub, J. Chem. Phys. **105**, 9546 (1996).
[25] J. Oviedo and R. E. Palmer, J. Chem. Phys. **117**, 9548 (2002).
[26] C. M. Chang and M. Y. Chou, Phys. Rev. Lett. **93**, 133401 (2004).
[27] E. Aprà, R. Ferrando, and A. Fortunelli, Phys. Rev. B **73**, 205414 (2006).
[28] R. C. Longo and L. J. Gallego, Phys. Rev. B **74**, 193409 (2006).
[29] M. Yang, K. A. Jackson, C. Koehler, T. Frauenheim, and J. Jellinek, J. Chem. Phys. **124**, 024308 (2006).
[30] L.-L. Wang and D. D. Johnson, Phys. Rev. B **75**, 235405 (2007).
[31] M. Pereiro, D. Baldomir, and J. E. Arias, Phys. Rev. A **75**, 063204 (2007).
[32] C. H. Hu, C. Chizallet, H. Toulhoat, and P. Raybaud, Phys. Rev. B **79**, 195416 (2009).
[33] F. Aguilera-Granja, A. García-Fuente, and A. Vega, Phys. Rev. B **78**, 134425 (2008).
[34] J. P. Chou, H. Y. T. Chen, C. R. Hsing, C. M. Chang, C. Cheng, and C. M. Wei, Phys. Rev. B **80**, 165412 (2009).
[35] M. J. Piotrowski, P. Piquini, and J. L. F. Da Silva, Phys. Rev. B **81**, 155446 (2010).
[36] J. P. Chou, C. R. Hsing, C. Cheng, and C. M. Chang, J. Phys. Condens. Matter **25**, 125305 (2013).
[37] S. Datta, A. K. Raychaudhuri, and T. Saha-Dasgupta, J. Chem. Phys. **146**, 164301 (2017).
[38] F. Baletto and R. Ferrando, Rev. Mod. Phys. **77**, 371 (2005).
[39] T. P. Martin, Phys. Rep. **273**, 199 (1996).
[40] E. K. Parks, L. Zhu, J. Ho, and S. J. Riley, J. Chem. Phys. **102**, 7377 (1995).
[41] E. K. Parks, G. C. Nieman, K. P. Kerns, and S. J. Riley, J. Chem. Phys. **107**, 1861 (1997).
[42] E. K. Parks, G. C. Nieman, K. P. Kerns, and S. J. Riley, J. Chem. Phys. **108**, 3731 (1998).
[43] E. K. Parks, K. P. Kerns, and S. J. Riley, Chem. Phys. **262**, 151 (2000).
[44] C. R. Henry, Surf. Sci. Rep. **31**, 231 (1998).
[45] M. Valden, X. Lai, and D. W. Goodman, Science **281**, 1647 (1998).
[46] S. H. Joo, S. J. Choi, I. Oh, J. Kwak, Z. Liu, O. Terasaki, and R. Ryoo, Nature (London) **412**, 169 (2001).
[47] P. Entel, M. E. Gruner, G. Rollmann, A. Hucht, S. Sahoo, A. T. Zayak, H. C. Herper, and A. Dannenberg, Philos. Mag. **88**, 2725 (2008).
[48] J. A. Elliott, M. Hamm, and Y. Shibuta, J. Chem. Phys. **130**, 034704 (2009).

[49] S.-J. Park, T. A. Taton, and C. A. Mirkin, Science **295**, 1503 (2002).
[50] C. A. Mirkin, R. L. Letsinger, R. C. Mucic, and J. J. Storhof, Nature (London) **382**, 607 (1996).
[51] M. D. Wolf and U. Landman, J. Phys. Chem. A **102**, 6129 (1998).
[52] R. Poteau and G. M. Pastor, Eur. Phys. J. D **9**, 235 (1999).
[53] J.-O. Joswig and M. Springborg, Phys. Rev. B **68**, 085408 (2003).
[54] S. Darby, T. V. Mortimer-Jones, R. L. Johnston, and C. Roberts, J. Chem. Phys. **116**, 1536 (2002).
[55] T. Lazauskas, A. A. Sokol, and S. M. Woodley, Nanoscale **9**, 3850 (2017).
[56] M. Atiş, H. Aktaş, and Z. B. Güvenç, Modell. Simul. Mater. Sci. Eng. **13**, 1411 (2005).
[57] K. Michaelian, N. Rendón, and I. L. Garzón, Phys. Rev. B **60**, 2000 (1999).
[58] J. García-Rodeja, C. Rey, L. J. Gallego, and J. A. Alonso, Phys. Rev. B **49**, 8495 (1994).
[59] S. Özçelik and Z. B. Güvenç, Surf. Sci. **532**, 312 (2003).
[60] Ş. Erkoç and R. Shaltaf, Phys. Rev. A **60**, 3053 (1999).
[61] J. Jellinek and I. L. Garzón, Z. Phys. D **20**, 239 (1991).
[62] C. Rey, J. García-Rodeja, and L. J. Gallego, Phys. Rev. B **54**, 2942 (1996).
[63] C. Luo, Modell. Simul. Mater. Sci. Eng. **8**, 95 (2000).
[64] M. Kabir, A. Mookerjee, and A. K. Bhattacharya, Phys. Rev. A **69**, 043203 (2004).
[65] M. W. Finnis and J. E. Sinclair, Philos. Mag. A **50**, 45 (1984).
[66] M. W. Finnis and J. E. Sinclair, Philos. Mag. A **53**, 161 (1986).
[67] A. P. Sutton and J. Chen, Philos. Mag. Lett. **61**, 139 (1990).
[68] I. L. Garzón and J. Jellinek, Z. Phys. D **20**, 235 (1991).
[69] A. Posada-Amarillas and I. L. Garzón, Phys. Rev. B **54**, 10362 (1996).
[70] H. Häkkinen, M. Moseler, and U. Landman, Phys. Rev. Lett. **89**, 033401 (2002).
[71] E. M. Fernández, J. M. Soler, I. L. Garzón, and L. C. Balbás, Phys. Rev. B **70**, 165403 (2004).
[72] G. Kresse and J. Furthmüller, Phys. Rev. B **54**, 11169 (1996).
[73] A buckled biplanar (BBP) structure consists of two planes: a hexagonal plane with a central atom and a square with two flanking atoms between the hexagonal layer and the square. In a hexagonal bilayer (HBL) structure, the square with two flanking atoms is replaced by an additional hexagonal plane. Depending on the total energy of the structures, the hexagon(s) and the square can be distorted with a varying degree of buckling of the planes.
[74] L. Mitas, J. C. Grossman, I. Stich, and J. Tobik, Phys. Rev. Lett. **84**, 1479 (2000).
[75] C. Pangali, M. Rao, and B. J. Berne, Chem. Phys. Lett. **55**, 413 (1978).
[76] Our choice of δr_i^{mn} from a uniform random distribution eliminates the coupling between the terms on the right-hand side of Eq. (7), as mentioned in the context of Brownian dynamics simulations. However, this has no direct bearing on the present FMC simulations as the primary goal of our work is to minimize the total energy of the clusters.
[77] W. Kohn and L. J. Sham, Phys. Rev. **140**, A1133 (1965).
[78] J. P. Perdew, K. Burke, and M. Ernzerhof, Phys. Rev. Lett. **77**, 3865 (1996).
[79] L. Kleinman and D. M. Bylander, Phys. Rev. Lett. **48**, 1425 (1982).
[80] R. Car and M. Parrinello, Phys. Rev. Lett. **55**, 2471 (1985).
[81] For a list of putative global minima and the corresponding structure of a number of clusters, visit the Cambridge Cluster Database at http://www-wales.ch.cam.ac.uk/CCD.html.
[82] G. L. Gutsev, C. W. Weatherford, K. G. Belay, B. R. Ramachandran, and P. Jena, J. Chem. Phys. **138**, 164303 (2013).
[83] M. Wu, A. K. Kandalam, G. L. Gutsev, and P. Jena, Phys. Rev. B **86**, 174410 (2012).
[84] M. J. Frisch, G. W. Trucks, H. B. Schlegel, G. E. Scuseria, M. A. Robb, J. R. Cheeseman, G. Scalmani, V. Barone, B. Mennucci, G. A. Petersson, H. Nakatsuji, M. Caricato, X. Li, H. P. Hratchian, A. F. Izmaylov, J. Bloino, G. Zheng, J. L. Sonnenberg, M. Hada, M. Ehara, K. Toyota, R. Fukuda, J. Hasegawa, M. Ishida, T. Nakajima, Y. Honda, O. Kitao, H. Nakai, T. Vreven, J. A. Montgomery, Jr., J. E. Peralta, F. Ogliaro, M. Bearpark, J. J. Heyd, E. Brothers, K. N. Kudin, V. N. Staroverov, R. Kobayashi, J. Normand, K. Raghavachari, A. Rendell, J. C. Burant, S. S. Iyengar, J. Tomasi, M. Cossi, N. Rega, J. M. Millam, M. Klene, J. E. Knox, J. B. Cross, V. Bakken, C. Adamo, J. Jaramillo, R. Gomperts, R. E. Stratmann, O. Yazyev, A. J. Austin, R. Cammi, C. Pomelli, J. W. Ochterski, R. L. Martin, K. Morokuma, V. G. Zakrzewski, G. A. Voth, P. Salvador, J. J. Dannenberg, S. Dapprich, A. D. Daniels, Farkas, J. B. Foresman, J. V. Ortiz, J. Cioslowski, and D. J. Fox, *GAUSSIAN 09, revision E.01*, Gaussian Inc., Wallingford, CT, 2009.
[85] In computing the pair-correlation function of a cluster, using the conventional definition of the radial correlation between atoms, we have used a suitable bounding box to calculate the number density of the atoms. Since the number density is identical for both the FMC and CCD clusters, our results are not affected by any small variation or arbitrariness in the size of the bounding box.
[86] P. J. Steinhardt, D. R. Nelson, and M. Ronchetti, Phys. Rev. B **28**, 784 (1983).
[87] Given two units vectors **P** and **Q** in three-dimensional space, **P** can be aligned with **Q** by constructing a rotation axis along $\mathbf{P} \times \mathbf{Q}$ and rotating **P** by an angle $\theta = \cos^{-1}(\mathbf{P} \cdot \mathbf{Q})$. This axis-angle representation of vector rotation in three dimensions can be translated into appropriate Euler rotation matrices. For small systems, it is often convenient to employ directly the Rodrigues formula for rotation of a vector around a given axis in three dimensions.